Received: 30 August 2023 | Accepted: 13 March 2024

DOI: 10.1111/evj.14088

ORIGINAL ARTICLE

Equine Veterinary Journal WILEY

Low-field magnetic resonance imaging of sagittal groove disease of the proximal phalanx in non-racing sport horses

Josephine E. Faulkner[1] | Zoë Joostens[2] | Bart J. G. Broeckx[3] | Stijn Hauspie[2] | Tom Mariën[2] | Katrien Vanderperren[1]

[1]Department of Morphology, Imaging, Orthopaedics, Rehabilitation and Nutrition, Faculty of Veterinary Medicine, Ghent University, Merelbeke, Belgium

[2]Equitom Equine Clinic, Lummen, Belgium

[3]Department of Veterinary and Biosciences, Faculty of Veterinary Medicine, Ghent University, Merelbeke, Belgium

Correspondence
Josephine E. Faulkner, Department of Morphology, Imaging, Orthopaedics, Rehabilitation and Nutrition, Faculty of Veterinary Medicine, Ghent University, Salisburylaan 133, 9820 Merelbeke, Belgium.
Email: josie.faulkner@ugent.be

Abstract

Background: Injuries of the sagittal groove of the proximal phalanx (P1) in equine athletes are considered to predominantly occur due to chronic bone stress overload.

Objectives: To describe the range of abnormalities that is present in the sagittal groove in a large group of horses diagnosed with sagittal groove disease (SGD) on low-field MRI.

Study Design: Retrospective, cross-sectional.

Methods: Medical records were searched to identify initial MRI images of horses diagnosed with SGD and these were blindly evaluated using a semi-quantitative grading scheme and novel SGD MRI classification system reflecting potential pathways of pathological progression and severity of stress injury.

Results: A total of 132 limbs from 111 horses were included in the study; predominantly warmbloods competing in showjumping ($n = 83$) and dressage ($n = 18$). SGD MRI classifications were: 0 (normal, $n = 0$), 1 (small subchondral defect, $n = 2$), 2 (osseous densification, $n = 28$), 3 (subchondral microfissure with osseous densification, $n = 7$), 4 (bone oedema-like signal within the subchondral ± trabecular bone and ± subchondral microfissure or demineralisation, $n = 72$), 5 (incomplete macrofissure/fracture, $n = 23$) and 6 (complete fracture, $n = 0$). Classification 4c (bone oedema-like signal with demineralisation) and 5 had higher proportions in the plantar third of hindlimbs (3% and 10%, respectively) compared with forelimbs (0% and 0%, respectively). SGD classification and extent of bone oedema-like signal were not significantly different between lame ($n = 116$) and non-lame limbs ($n = 16$) (both $p > 0.05$). Periosteal new bone and oedema-like signal were identified (either confidently or suspected) at the dorsoproximal aspect of P1 in 25% and 39% of limbs, respectively.

Main Limitations: Inclusion via diagnoses in original MRI reports, variable clinical history, small size of some classification groups.

Conclusions: The presence or absence of lameness is not a dependable measure of the severity of SGD. The periosteal oedema-like signal of P1 has not previously been described in MRI of SGD and further supports the concept of bone stress injury.

KEYWORDS
bone stress, fissure, horse, P1, periostitis, subchondral bone

1 | INTRODUCTION

Sagittal groove (SG) injuries of the proximal phalanx (P1) are an increasingly recognised cause of lameness in equine athletes and early diagnosis can aid in optimising rehabilitation programs and prevention of further injury. Several publications have described the variable abnormal imaging features of the SG on radiography, magnetic resonance imaging (MRI), computed tomography (CT) and scintigraphy; where pathology included subchondral osseous densification (sclerosis), subchondral bone demineralisation (resorption), bone oedema-like lesions (bone marrow lesions), osseous cyst-like lesions, fissures and incomplete and complete fractures.[1–13] To date there are no studies evaluating the distribution of the type and severity of MRI findings in a large group of horses.

In many cases, sagittal groove disease (SGD) is considered to occur due to a maladaptive response to chronic bone stress overload and is suspected to be associated with repetitive hyperextension of the fetlock joint under loading.[2–6,9,11,14,15] MRI is a well-established modality for the assessment of bone stress injuries due to its ability to detect bone oedema-like signal and, in addition, osseous densification and degenerative joint disease can also be appreciated.[16] In human medicine, the Modified Fredericson MRI Classification System is used for categorising stress injuries of the tibia based on presence of periosteal oedema, bone marrow oedema and intracortical signal abnormality.[17] It reflects the pathological progression of this condition and this scheme is validated for use in predicting time to return to sports activity.[17,18] An MRI classification system has recently been proposed for SGD in equine athletes.[19]

The aims of this study were therefore (1) to describe the range of MRI abnormalities present in the SG in a large group of horses diagnosed with SGD at the initial MRI examination, and (2) to utilise an MRI classification system for SGD associated with chronic overload/stress injury that is based on similar conceptualisation of the Modified Fredericson MRI Classification System and adapted to reflect the articular nature of SGD in horses.

It was hypothesised that (a) a higher proportion of SGD would be encountered in the forelimbs of jumping horses and in the hindlimbs of horses that perform exclusively flatwork, (b) SG pathology would be most prevalent in a dorsal location in forelimbs and plantarly in hindlimbs, (c) periosteal new bone formation and periosteal oedema-like signal would be present at the dorsoproximal and/or palmaro/plantaroproximal aspects of P1 in a proportion of cases with SGD, further supporting the aetiological theory of bone stress injury, (d) SGD classification would not be associated with presence or absence of lameness, and (e) the extent of subchondral and trabecular bone oedema-like signal associated with the SG would be higher in lame horses than in non-lame horses.

2 | MATERIALS AND METHODS

2.1 | Case selection

The study was retrospective, descriptive and cross-sectional in design. Inclusion criteria were horses >1 year old which underwent low-field standing MRI examination of at least one fetlock at Equitom Equine Clinic between March 2014 and March 2023 and in which abnormalities of the P1 SG were diagnosed. Dates were selected to ensure the largest possible convenience sample, representing the full period of operational use of the standing MRI equipment at this facility at the time of the research investigation. Cases were found by keyword search of the archived MRI reports by one author (ZJ, ECVDI certified radiologist, Radiologist 1) using the terms 'P1', 'proximal phalanx', 'sagittal groove', 'sagittal groove disease', 'fissure' and 'incomplete fracture' and their equivalent terms in Dutch and French. The original reports were written predominantly by ECVDI-certified radiologists (2014–2023) and a small number were written by an experienced and competent diagnostic imaging veterinarian (2014–2018). In cases with serial MRI examinations, only the first MRI examination in which abnormalities of the SG were noted SGD was included in the study.

Clinical information as provided by the referring vet was collected and anonymised by Radiologist 1. Clinical information collected included the date of MRI examination, signalment (birth date, sex, breed), clinical history (athletic use, level of work, reason for MRI, duration of lameness, previous imaging examinations) and clinical examination findings (lame limb, severity, localising clinical signs such as fetlock joint distension, response to flexion, results of local anaesthetic blocks). Cases were categorised into two groups: horses presented due to lameness and those without lameness in which a SG lesion was detected or suspected on screening radiographic examination (e.g., pre-purchase examination, osteochondrosis screening). Lameness status was determined on the basis of clinical history and clinical examination findings from referring veterinarians. A standardised method of determining lameness was not used, but they were all at least visually assessed for lameness.

2.2 | MRI examination protocol

MRI studies were retrieved and anonymised by Radiologist 1. All cases had undergone examination of the fetlock with an open 0.27 T permanent magnetic resonance system (Hallmarq EQ2) under standing sedation (Supplementary Item 1).

2.3 | MRI evaluation

Images were graded by an ECVDI certified radiologist (JF, Radiologist 2) who was blinded to the horse signalment and clinical history. Cases were viewed using a DICOM viewer (Horos v.4.0.0 RC5, horosproject.org) in a random order (www.random.org/sequences/). The MRI sequences used for evaluation of the proximal phalanx were recorded and all available sequences were used for assessment. If a criterium was impossible to evaluate due to lack of appropriate sequences or excessive artefact, this was noted as 'cannot evaluate'. Examinations with insufficient sequences for adequate assessment of the majority of criteria were excluded on consensus agreement between Radiologist 1 and 2.

Once complete, Radiologist 2 reviewed the grading data alongside the original MRI reports to check for conflicting findings. Discrepancies regarding the presence or absence of lesions were recorded and later

evaluated by a second blinded EVCDI certified radiologist (KV, Radiologist 3) who made the deciding verdict (majority rule decision-making). In the case of a discrepancy in level of severity of a lesion, the images were re-examined and the grade according to the grading scheme took precedence over the term used in the original report. Discrepancies of this type were not chronicled.

2.3.1 | Semi-quantitative grading scheme

The SG was divided into three subregions: dorsal, middle and palmar/plantar thirds and each subregion was graded using a semi-quantitative scheme. Criteria were adapted from previous publications[2,10,16,19,20] and consideration was given to the reported ranges of subchondral bone thickness in P1 obtained from post-mortem specimens on microCT.[14] For each category the highest-ranked grade from the three subregions was assigned as the overall grade for that limb. The more detailed visual guide of the semi-quantitative scheme is presented in Supplementary Item 2.

Subchondral defects were defined as interruptions of the subchondral bone and graded: 0, absent; 1, minor defect; 2, microfissure; 3, short macrofissure; 4, long macrofissure/fracture; and further categorised as unipartite (singular lesion) or tripartite (three parallel dorsopalmarly/plantarly and proximodistally oriented defects/lines, typically two hyperintense lines flanking a hypointense line, considered similar to the 'chromosome-like' fissures reported in CT[2]). Subchondral demineralisations were defined as regions within the subchondral bone plate that were hyperintense on all sequences, without proximodistal linearity, and graded: 0, absent; 1, unipartite; 2, tripartite/'chromosome-like'.

Osseous densification was defined as abnormal low signal intensity of the subchondral and/or trabecular bone on T1-weighted (T1W) gradient recalled echo (GRE) and T2-weighted (T2W) fast spin echo (FSE) sequences and graded: 0, normal; 1, less than the depth of the SG; 2, extending up to the level of the physis/physeal scar; 3, extending into the diaphysis. Bone oedema-like signal was defined as hypointense signal on T1W GRE, hyperintensity on short tau inversion recovery (STIR) FSE, and intermediate or increased intensity on T2-weighted out-of-phase (T2*W) GRE with rim of hypointensity (fat water cancellation phenomenon). This was graded: 0, none; 1, subchondral bone plate only; 2, extending to the level of the physis/physeal scar; 3, extending into the diaphysis; 4, extending to the diaphysis with distal linear extension.

Mediolateral location of these lesions was recorded and the size of subchondral defects and demineralisations (mm) was measured in three planes (proximodistal × dorsopalmar/plantar × mediolateral (PrDi × DoP × ML)). Cartilage signal was not included in the assessment as this is not reliable when using a standing low-field magnetic resonance system.[21]

Presence of periosteal new bone formation and periosteal oedema-like signal (Figure 1) were assessed at the dorsoproximal and palmar/plantaroproximal aspects of P1. Intraosseous vascular channels within the proximal aspect of P1 were subjectively graded as normal or increased.

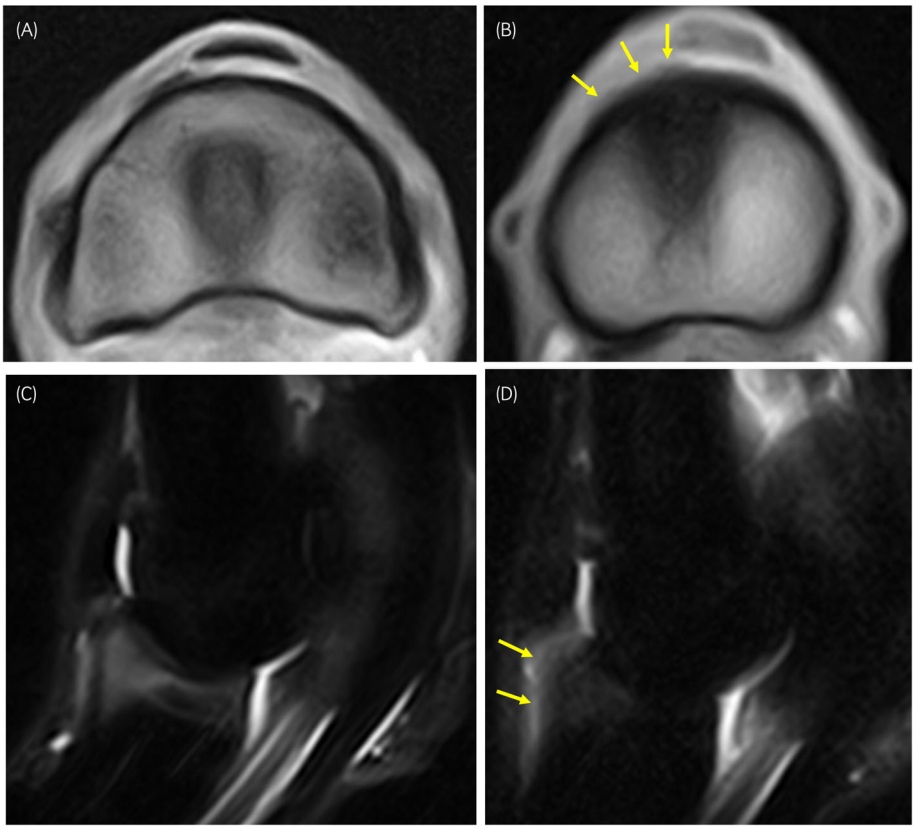

FIGURE 1 (A, B) Magnetic resonance imaging (MRI) transverse T1W GRE image of the proximal aspect of the proximal phalanx in limbs with SGD with (A) absence of periosteal new bone with visualisation of the distal aspect of the lateral digital extensor tendon, and (B) presence of dorsoproximolateral periosteal new bone (arrows; slice located further distally than in A); (C, D) MRI sagittal plane STIR FSE images of the fetlock in limbs with SGD both showing increased trabecular bone oedema-like signal and with (C) absence of periosteal oedema-like signal at the dorsoproximal aspect of the proximal phalanx, and (D) presence of periosteal oedema-like signal at the dorsoproximal aspect of the proximal phalanx (arrows). STIR FSE, short tau inversion recovery fast spin echo; T1W GRE, T1-weighted gradient recalled echo.

2.3.2 | MRI classification system for sagittal groove disease

An SGD MRI classification system formulated to reflect suspected pathways of pathological progression and severity of chronic overload/stress injury in this region was used, consisting of classification groups 0–6, with several sub-classifications (a, b and c) (Table 1, Figures 2 and 3).[17–19] The results of the above-described semi-quantitative grading scheme were used to determine the classification for each subregion (dorsal, middle and palmar/plantar) and an overall SG MRI classification was assigned to the limb using the highest ranking from the three subregions.

2.4 | Data analysis

Descriptive analysis was performed by JF (Microsoft Excel Version 16.72, Microsoft Corporation). The statistical analysis was conducted

TABLE 1 Sagittal groove disease MRI classification system, formulated to reflect the suspected pathways of pathological progression of chronic overload/stress injury in this region.

SGD MRI classification	Sub-classifications and description of key osseous changes in the SG	Absent concurrent features	Potential concurrent features
0 Normal	No abnormalities	N/A	N/A
1 Small subchondral defect	(a) Minor, shallow defect in the chondro-osseous junction (typically ≤1 mm depth ± visible in only one slice) (b) Microfissure (proximodistally-oriented, narrow, linear defect in the chondro-osseous junction that is contained within the subchondral bone plate, ≤3 mm length)	Demineralisation, osseous densification, bone oedema-like signal	N/A
2 Osseous densification	(a) Mild osseous densification of the subchondral ± trabecular bone, not extending to the proximal physis/physeal scar (proximodistal extent less than the equivalent depth of the SG) (b) Moderate to severe osseous densification of the subchondral ± trabecular bone, extending to or beyond the proximal physis/physeal scar (proximodistal distance greater than one times the depth of the SG)	Microfissure, demineralisation, bone oedema-like signal	Minor subchondral defect
3 Subchondral microfissure with osseous densification	(a) Subchondral microfissure (≤3 mm length) with mild osseous densification (does not reach the proximal physis/physeal scar) (b) Subchondral microfissure (≤3 mm length) with moderate to severe osseous densification (extending to or beyond the proximal physis/physeal scar)	Subchondral demineralisation or bone oedema-like signal	
4 Bone oedema-like signal within the subchondral ± trabecular bone	(a) Bone oedema-like signal within the subchondral ± trabecular bone	Microfissure, demineralisation	Minor subchondral defect, osseous densification of any extent
	(b) Bone oedema-like signal within the subchondral ± trabecular bone *with* microfissure (short proximodistally-oriented, narrow, linear defect contained within the subchondral bone plate (≤3 mm))	Demineralisation	Osseous densification of any extent
	(c) Bone oedema-like signal within the subchondral ± trabecular bone *with* subchondral demineralisation (unipartite or tripartite regions of demineralisation/resorption within the subchondral bone plate)		Microfissure, osseous densification of any extent
5 Incomplete macrofissure/fracture	Proximodistally oriented linear signal abnormality (>3 mm length; unipartite or tripartite configuration) extending through the subchondral bone and terminating within the trabecular bone	N/A	Demineralisation, osseous densification or bone oedema-like signal of any extent
6 Complete fracture	Proximodistally oriented linear signal abnormality extending through the subchondral and trabecular bone and exiting at the diaphyseal cortex or distal subchondral bone plate with the creation of two or more fragments	N/A	Demineralisation, osseous densification or bone oedema-like signal of any extent.

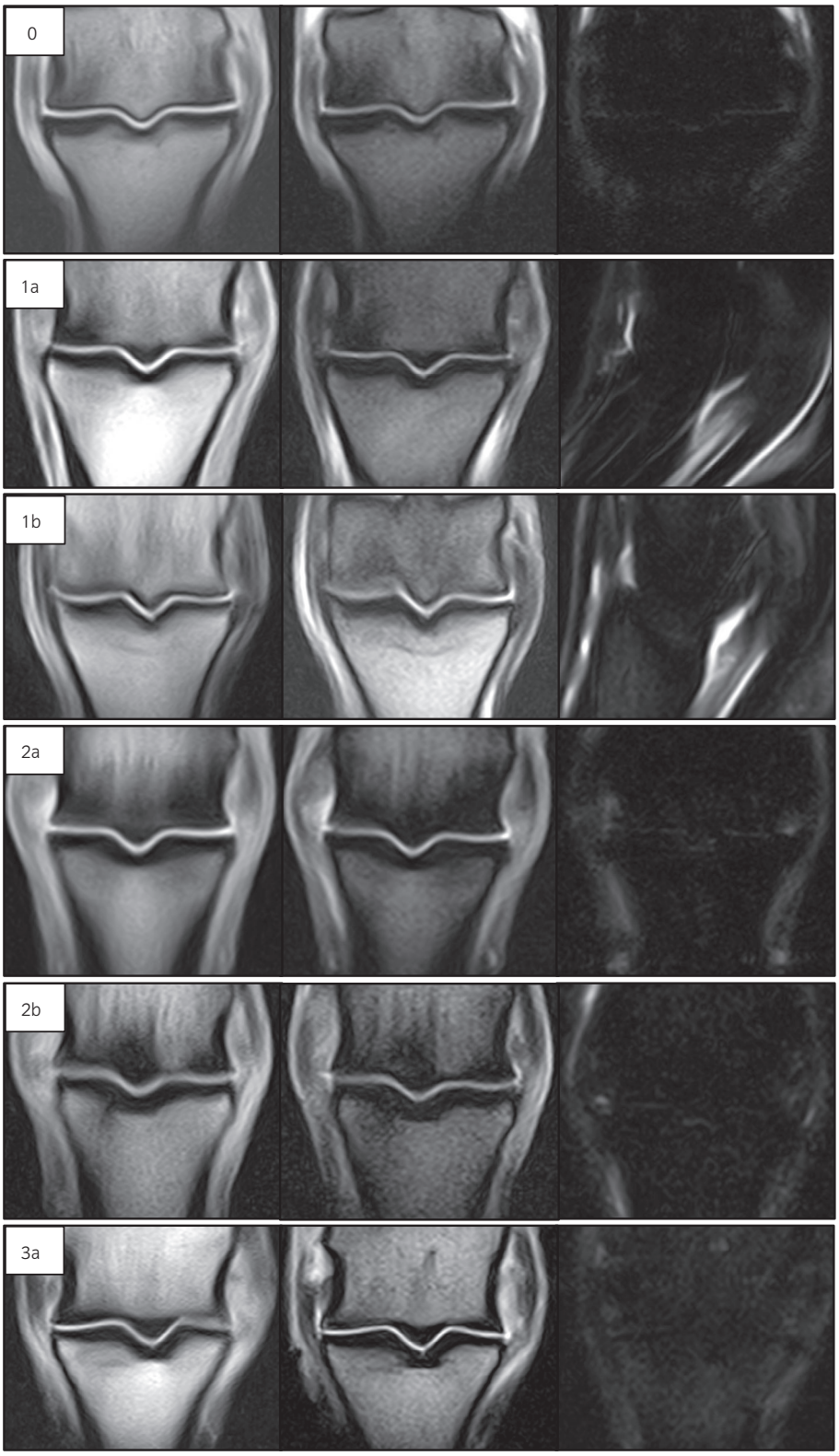

FIGURE 2 Example images of sagittal groove disease magnetic resonance imaging classification types 0, 1a, 1b, 2a, 2c, 2b and 3a in T1W GRE frontal (left), T2*W GRE frontal (middle), STIR FSE frontal or sagittal (right) planes. No examples with 3b were identified in the population examined, even within individual subregions. STIR FSE, short tau inversion recovery fast spin echo; T1W GRE, T1-weighted gradient recalled echo; T2*W GRE, T2-weighted out-of-phase gradient recalled echo.

by BB (R Version 4.2.2, R Foundation for Statistical Computing). The association between categorical variables was evaluated with Fisher's exact test. To correct for multiple testing, a Holm–Bonferroni correction was applied. Any semi-quantitative grading criteria that were allocated as 'cannot evaluate' were excluded from statistical analysis. Analyses of SGD MRI classifications were performed for both the main classification groups as well as for sub-classifications. Limbs were excluded from analyses comparing lame and non-lame limbs if the lameness status of the limb was not explicitly stated in the clinical notes. Significance was set at $\alpha < 0.05$.

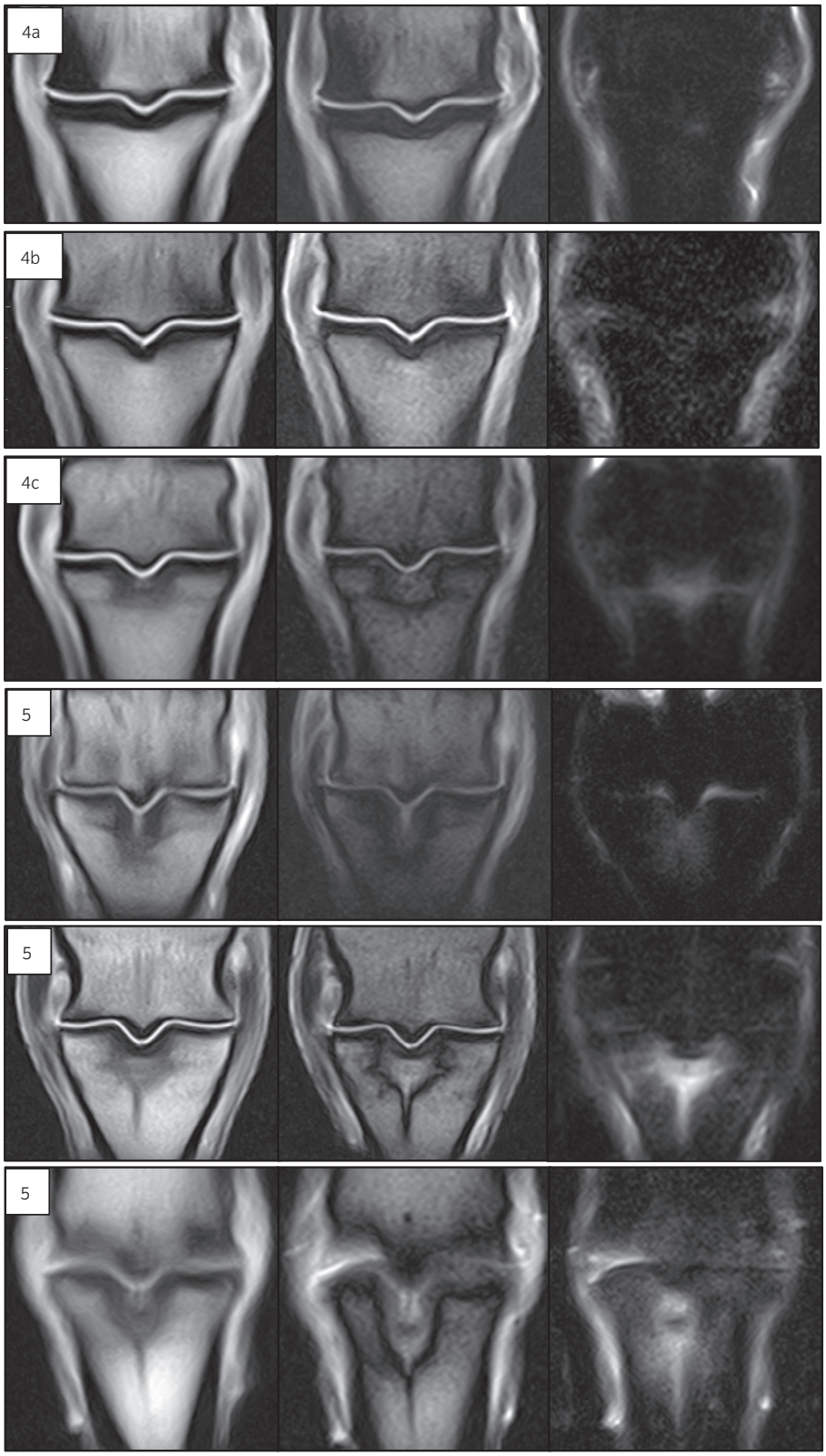

FIGURE 3 Example images of sagittal groove disease magnetic resonance imaging classification types 4a, 4b, 4c and three variants of 5 in T1W GRE frontal (left), T2*W GRE frontal (middle), STIR FSE frontal (right) planes. The first two variants of classification 5 have a unipartite configuration and the third has a tripartite appearance. STIR FSE, short tau inversion recovery fast spin echo; T1W GRE, T1-weighted gradient recalled echo; T2*W GRE, T2-weighted out-of-phase gradient recalled echo.

3 | RESULTS

3.1 | Horses

During the study period, a total of 1590 fetlock MRI scans were acquired at Equitom Equine Clinic. Search of the archived MRI reports identified 112 horses with SGD. One horse was excluded due to insufficient sequences resulting in inclusion of 111 horses in the study (Figure 4). There were 55 mares, 9 stallions and 47 geldings. Mean ± SD age was 9.8 ± 3.1 years (range 1.3–18.5 years). Breeds included 104 warmbloods, 3 ponies, 2 Quarter Horses, 1 Arabian and 1 Friesian. The disciplines of the horses were 83 showjumping (FEI 5* ($n = 21$),

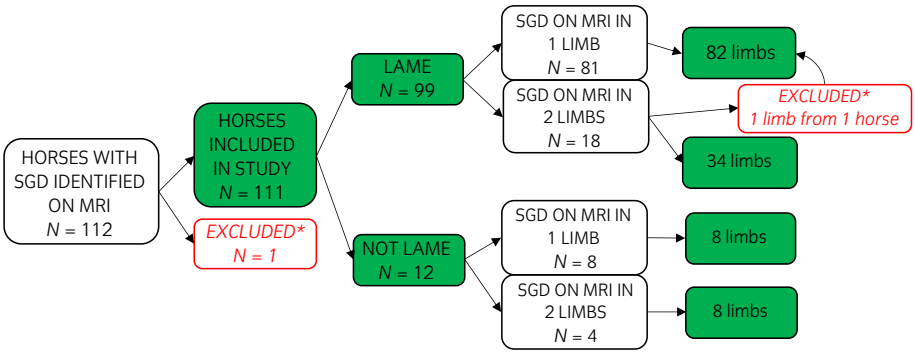

FIGURE 4 Flowchart overview of horses and limbs included in the study. *, excluded due to insufficient sequences; MRI, magnetic resonance imaging; N, number of horses; SGD, sagittal groove disease.

4* ($n = 12$), 3* ($n = 19$), 2* ($n = 9$), 1* ($n = 9$), National level, for example, Young Horse Championship ($n = 13$)), 18 dressage (FEI CDI 5* ($n = 3$), 3* ($n = 4$), 1* ($n = 2$), National level ($n = 7$), CDI 5* children's competition ($n = 2$)), 5 leisure, 2 western (FEI 5* reining ($n = 1$), National level ($n = 1$)), 1 eventing (FEI 4*), 1 driving (FEI 4*) and 1 showing. Ninety-nine horses were lame, with a mean ± SD age of 10.0 ± 3.1 years (range 1.3–18.5 years). Twelve horses were not lame, with mean ± SD age of 8.8 ± 3.1 years (range 4.9–15.4 years). The amount of clinical information available varied markedly between horses and a summary of these additional findings are presented in Supplementary Item 3.

3.2 | MRI acquisition

Horses underwent MRI examination of one fetlock ($n = 88$), two fetlocks ($n = 22$) or three fetlocks ($n = 1$). SGD was diagnosed in one limb in 89 horses and two limbs in 22 horses. One limb from a horse diagnosed with bilateral forelimb SGD was excluded from the study due to insufficient sequences (Figure 4). Ultimately a total of 132 limbs diagnosed with SGD were included in the study: 44 left forelimb (LF), 59 right forelimb (RF), 17 left hindlimb (LH), 12 right hindlimb (RH). This included cases with bilateral forelimbs (18 horses) and cases with one forelimb and one hindlimb (3 horses: RF, RH ($n = 2$); RF, LH ($n = 1$)).

Sagittal groove disease was diagnosed more commonly in forelimbs than hindlimbs in all disciplines: showjumping (73 forelimbs, 21 hindlimbs), dressage (18 forelimbs, 6 hindlimbs), leisure (5 forelimbs, 2 hindlimbs), western (3 forelimbs), eventing (2 forelimbs), driving (1 forelimb) and showing (1 forelimb). When comparing horses that jumped (showjumping and eventing) with those that did flatwork exclusively (dressage, western, showing and driving) there was no significant difference between the relative proportions of forelimbs and hindlimbs affected (78.1% forelimbs, 21.9% hindlimbs and 79.3% forelimbs, 20.7% hindlimbs, respectively; $p > 0.9$).

Choice of MRI sequences performed on the fetlock varied between cases (Supplementary Item 1). Other regions scanned during the same investigation of each limb included the foot ($n = 66$), pastern ($n = 39$), metacarpus/metatarsus ($n = 17$) and carpus/tarsus ($n = 5$).

3.3 | MRI evaluation

There were 14 discrepancies between the grading and the original report in terms of identification of lesions (subchondral defect ($n = 2$), subchondral demineralisation ($n = 2$), osseous densification ($n = 1$) and bone oedema-like signal ($n = 9$)). Radiologist 3 agreed with the assessment of Radiologist 2 in 10 cases and agreed with the original report in four cases. The grades were altered accordingly before data analysis.

3.3.1 | Semi-quantitative grading scheme

Overall grades of subchondral defect for the SG were: grade 0 (absent; $n = 24$), grade 1 (minor defect; $n = 48$), grade 2 (microfissure; $n = 37$), grade 3 (short macrofissure; $n = 20$), grade 4 (long macrofissure/fracture; $n = 3$). Mean ± sd dimensions (PrDi × DoP × ML) were: grade 1 (1.1 ± 0.2 × 10.4 ± 7.3 × 1.3 ± 0.5 mm), grade 2 (1.8 ± 0.8 × 12.8 ± 6.4 × 1.2 ± 0.6 mm), grade 3 (6.3 ± 2.1 × 16.8 ± 8.6 × 1.2 ± 0.8 mm) and grade 4 (25.7 ± 15 × 28.3 ± 5.1 × 2.3 ± 2.3 mm).

The majority of subchondral defects were located mid-sagittally: grade 1 (84.3%), grade 2 (60.4%), grade 3 (80%) and grade 4 (100%). The remaining defects were located at the lateral margin of the mid-sagittal zone (grade 1 (7.1%), grade 2 (31.7%) and grade 3 (17.1%)), medial margin of the mid-sagittal zone (grade 1 (8.6%), grade 2 (4.8%) and grade 3 (2.9%)) and medial sloping parasagittal region (grade 2 (3.2%)). A tripartite morphology of subchondral defect was only present in the mid-sagittal location: grade 2 (4.8%), grade 3 (28.6%) and grade 4 (33.3%). The remainder of subchondral defects were unipartite.

Overall grades of subchondral demineralisation were: grade 0 (absent; $n = 117$), grade 1 (unipartite; $n = 9$) and grade 2 (tripartite; $n = 6$). Mean ± SD dimensions (PrDi × DoP × ML) were 4.1 ± 2.8 × 10.4 ± 5.7 × 4.3 ± 2.3 mm. Demineralisations were more often located in the mid-sagittal zone ($n = 9$), than in the medial ($n = 5$) or lateral ($n = 1$) parasagittal sloping zones. Unipartite demineralisation sometimes had concurrent microfissure ($n = 2$) or short macrofissure ($n = 1$). Tripartite demineralisation always had a concurrent microfissure ($n = 2$) or macrofissure ($n = 4$) and sometimes flanked the medial and lateral margins of the defect. An osseous cyst-like lesion (OCLL; 3 × 4 × 2mm) was identified in the lateral parasagittal subchondral bone in the middle subregion in one forelimb. There were two

additional small OCLLs within the P1 medial fovea and the third metacarpal condyle of the same limb.

Overall grades of osseous densification were: grade 0 ($n = 6$), grade 1 ($n = 97$), grade 2 ($n = 23$) and grade 3 ($n = 6$). Densification was centred mid-sagittal (64.4%), toward the medial aspect (29.1%) or toward the lateral aspect (6.5%).

Overall grades of bone oedema-like signal were: grade 0 ($n = 37$), grade 1 ($n = 38$), grade 2 ($n = 37$), grade 3 ($n = 17$) and grade 4 ($n = 3$). Bone oedema-like signal was centred mid-sagittal (68.5%), toward the medial aspect (21.7%) or toward the lateral aspect (9.8%). There was no significant difference gradings of bone oedema-like signal between lame and non-lame horses ($p = 0.4$).

The distribution of grades of subchondral defects, subchondral demineralisation, osseous densification and bone oedema-like signal grades according to subregion are shown in Figure 5.

Periosteal new bone formation was identified more often dorsoproximally (confidently identified, $n = 10$; suspected, $n = 22$) than palmaro/plantaroproximally (confidently identified, $n = 1$). Periosteal oedema-like signal was identified more often dorsally (confidently identified, $n = 27$; suspected, $n = 25$) than palmarly/plantarly (confidently identified, $n = 2$; suspected, $n = 3$). All limbs with confidently identified dorsal periosteal new bone also had confidently identified periosteal oedema-like signal ($n = 10/10$). At the one site of confidently identified palmar/plantar periosteal new bone, there was suspected periosteal oedema-like signal ($n = 1/1$). Conversely, limbs with confidently identified dorsal periosteal oedema-like signal only had periosteal new bone identified in a portion of cases (confident identification, $n = 10/27$; suspected, $n = 5/27$; not identified, $n = 12/27$) and palmar/plantarly it was not identified in either case ($n = 2/2$).

The proportions of lame limbs with confidently identified or suspected dorsal periosteal new bone (8.9% and 19.6%, respectively) were higher than in limbs from non-lame horses (0% and 0%, respectively) but the difference was not statistically significant ($p = 0.07$). Similarly, the proportions of lame limbs with confidently identified or suspected dorsal periosteal oedema-like signal (22.7% and 20.9%, respectively) were higher than in non-lame limbs (13.3% and 6.7%, respectively) but the difference was not statistically significant ($p = 0.3$).

Increased vascularisation was present in the proximal aspect of P1 in 28% of limbs and absent in 72%. Limbs with SGD classification 5 had the highest proportion with increased vascularisation (65% of limbs).

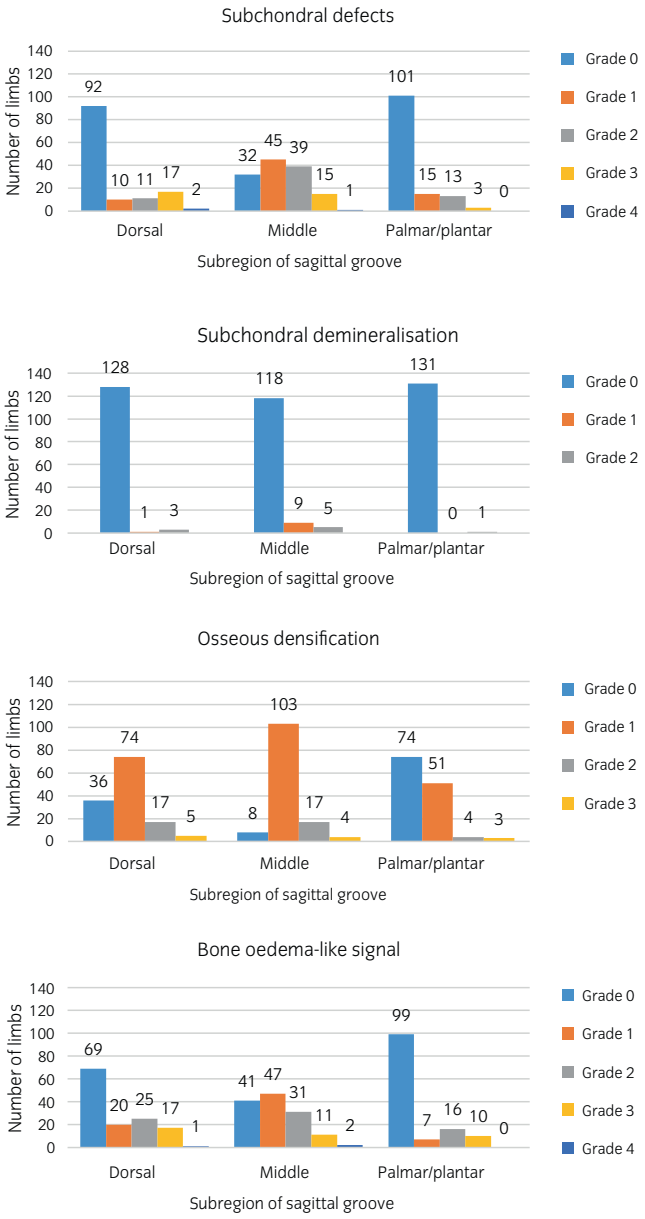

FIGURE 5 Bar charts showing distribution of grades of subchondral defects, subchondral demineralisation, osseous densification and bone oedema-like signal from the semi-quantitative grading scheme across the three subregions of the sagittal groove in 132 limbs diagnosed with sagittal groove disease on magnetic resonance imaging.

3.3.2 | Sagittal groove disease MRI classification system

Overall SGD MRI classifications were: 1a ($n = 2$), 2a ($n = 27$), 2b ($n = 1$), 3a ($n = 7$), 4a ($n = 36$), 4b ($n = 26$), 4c ($n = 10$) and 5 ($n = 23$). The distribution of semi-quantitative gradings relative to classification is shown in Supplementary Item 4. No limbs had overall classification 0, 1b, 3b or 6 and no subregions had classification 0, 3b or 6. In the horses with bilateral forelimb SGD identified on MRI, the sub-classification was the same in both limbs in 7 horses and different in 11 horses.

The distribution of classifications in forelimbs and hindlimbs is shown in Figure 6 and sub-classifications in Supplementary Item 5. When comparing the classifications in the dorsal, middle and palmar/plantar thirds of the SG between forelimbs and hindlimbs there was no significant difference ($p = 0.1$, $p = 0.06$ and $p = 0.09$ respectively). For sub-classifications, those in the dorsal third of the SG were not significantly different when compared between forelimbs and hindlimbs ($p = 0.4$) while those in the middle and palmar/plantar thirds

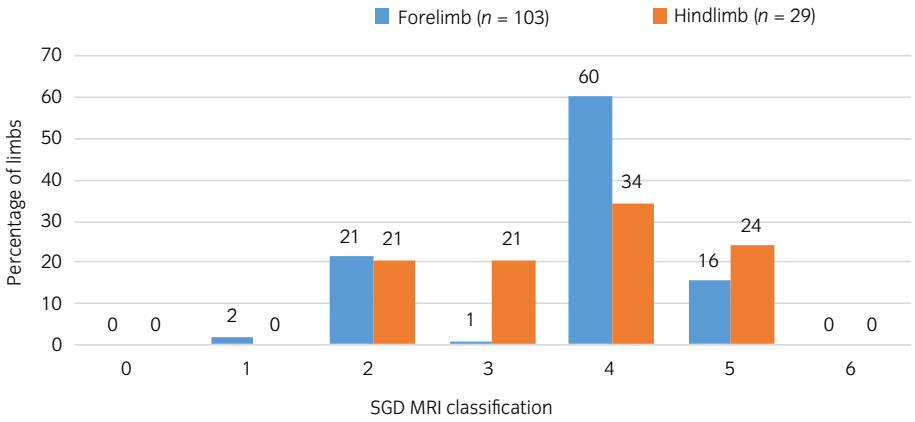

FIGURE 6 Bar charts showing comparison of the percentages of sagittal groove disease (SGD) magnetic resonance imaging (MRI) classification in 105 forelimbs and 29 hindlimbs with a diagnosis of SGD on MRI.

TABLE 2 Presence or absence of lameness prior to MRI referral versus sagittal groove disease MRI classification.

	Number of limbs (percentage)	
SGD MRI classification	Lame[a]	Not lame
0	0 (0.0%)	0 (0%)
1a	2 (1.8%)	0 (0%)
1b	0 (0.0%)	0 (0%)
2a	22 (19.5%)	4 (25%)
2b	1 (0.9%)	0 (0%)
3a	5 (4.4%)	2 (13%)
3b	0 (0.0%)	0 (0.0%)
4a	29 (25.7%)	5 (31%)
4b	22 (19.5%)	4 (25%)
4c	10 (8.8%)	0 (0%)
5	22 (19.5%)	1 (6%)
6	0 (0.0%)	0 (0%)
Total	113 (100%)	16 (100%)

[a]Three limbs of lame horses excluded due to absence of explicit detail of lameness status of limbs in the clinical notes.

were significantly different between forelimbs and hindlimbs ($p = 0.01$ and $p = 0.001$, respectively).

The MRI SGD classifications for lame and non-lame limbs are shown in Table 2 (three limbs were excluded from analysis due to absence of explicit detail of lameness status of limbs in the clinical notes). There was no significant difference in classification or sub-classifications between lame and non-lame limbs ($p = 0.4$ and $p = 0.6$, respectively).

4 | DISCUSSION

The SGD MRI classification system was successfully applied to all limbs. As expected, due to the inclusion criteria, no limbs were classified as 0 (normal). Classification 1 (small subchondral defect) was infrequently present and it is possible that these types may be underrepresented in the sample. Small subchondral bone defects can easily be missed on low-field MRI due to volume averaging and limits of resolution, or may be discounted as pathology and rather viewed as an anatomical variant during interpretation due to lack of concurrent densification or bone oedema-like signal. No limbs were classed as 1b (microfissure without other changes), and a reason for this may be that visible microfissures tend to be associated with concurrent osseous densification and/or bone oedema-like signal. Classification 2 (osseous densification) was assigned to a large number of limbs with similar relative proportions in forelimbs and hindlimbs. The vast majority were 2a (mild osseous densification) and authors consider that these are likely to represent non-pathological adaptive exercise-induced modelling. One forelimb was classified as 2b (moderate to severe osseous densification), with osseous densification reaching the level of the proximal physeal scar at the lateral aspect. Densification to this extent was more frequently associated with classification types 4a and higher therefore it is postulated that it may have resulted from a previous healed fissure.

All limbs with classification 3 were 3a (subchondral microfissure with mild osseous densification). This classification was proportionally more common in hindlimbs with the microfissure present in the middle third of the SG in the majority of instances. Likewise, microfissures in 4b (subchondral microfissure with bone oedema-like signal) were most frequently located in the middle subregion, however, this classification was more common in forelimbs. It is unknown whether these small subchondral microfissures should be regarded as a benign subchondral irregularity of developmental origin,[22] an anatomical variant that predisposes to more substantial pathology or whether they are an injury resulting from chronic overload or a previous supraphysiological traumatic event. Recent research showed that microscopic scores of subchondral bone sclerosis, microcracks, and collapse were significantly higher in locations with CT-identified fissures, suggestive of fatigue injuries.[23] No cases were classified as 3b (subchondral microfissure with moderate to severe osseous densification) as all microfissures with densification extending to or past the physeal scar also had associated bone oedema-like signal. The authors suspect that future research will support the merging of classification types 1b, 2b and 3b with their counterparts 1a, 2a and 3a, to simplify the classification system

(i.e., resulting classification groups 0, 1, 2, 3, 4a, 4b, 4c, 5, 6). Verification of a condensed version of the classification system will be important if it is to be effectively used in clinical practice.

The most prevalent classification was 4 (bone oedema-like signal within the subchondral ± trabecular bone) and more specifically 4a (bone oedema-like signal within the subchondral ± trabecular bone). 4a was proportionally more common in forelimbs and most often affected the dorsal and middle subregions of the SG, consistent with previous findings.[5] In 64% of limbs with 4a, the bone oedema-like signal was confined to the subchondral bone plate, and never extended to or past the physeal scar, contrasting with 4b, 4c (subchondral demineralisation with bone oedema-like signal) and 5 (macrofissure) in which it sometimes extended into the diaphysis. The importance of small amounts of bone oedema-like signal of the SG on low-field MRI is not known and longitudinal studies may provide more information on clinical consequences. Similarly, the clinical significance of bone marrow lesions in the distal condyles of the third metacarpal bone in sports and pleasure horses is still unclear as the severity of bone marrow lesions was shown not to be significantly associated with lameness nor with the type or level of activity.[24] The present study did not consider thin linear T2*W GRE hyperintensities within the subchondral bone plate without concurring T1W GRE or STIR FSE signal change to be increased bone oedema-like signal. These features are frequently visible in thick dense bone and they closely paralleled the anatomical contour of the articular surface, therefore most likely representing Gibbs or truncation artefact which occur as a result of under-sampling of data at interfaces of high and low signal intensity.[25] High-field MRI and/or histological examination would be required to confirm this assumption.

In horses classified as 4c, demineralisations were most common in the middle subregion of the SG in both forelimbs and hindlimbs. Although previously sometimes described as osseous cyst-like lesions due to their appearance on dorsopalmar/plantar radiographs, these demineralised regions represent sites of resorption and often extend in a dorsopalmar/plantar direction along the SG.[1,2] There was a concurrent microfissure or macrofissure in the SG of 33% of limbs with unipartite demineralisation and 100% of limbs with tripartite demineralisations. It is suspected that in cases of demineralisation without a visible micro- or macrofissure there is likely to be subchondral or trabecular microtrauma that is not appreciable on low-field MRI. Therefore, it is proposed that subchondral demineralisations should be considered prodromal or imminent fissure/fracture pathology. Future research is required to determine whether the prognosis for classifications 4a, 4b and 4c differ, and whether they should remain as separate classifications or could be merged.

Consistent with previous research, classification 5 in forelimbs showed a predisposition to the dorsal and middle subregions and never involved the palmar third of the SG.[2,5,9,20] Macrofissures in the hindlimbs were most frequently located in the dorsal and middle subregions but in three limbs they extended into the plantar third, involving all three subregions of the SG in these cases. Stress fractures and fissures are typically described as being hypointense on T1W and T2W images with surrounding bone oedema-like signal[26] and this was the case for some SG fissures in this study. However, other fissure lines were hyperintense and widened. The authors suggest that differing signal intensities and widths may represent different phases of fissure formation and healing, and be related to the amount of osseous microtrauma, oedema, osseous resorption, fibrosis and haemorrhage. It has previously been observed that some short, incomplete sagittal fractures which have been treated conservatively have a non-union at the joint surface that appears hyperintense on all sequences.[27] Some fissures had a single linear configuration and others a tripartite appearance (Figure 3), which may either represent two parallel fracture lines with resorptive margins as has been shown in CT previously or two regions of resorption flanking a hypointense fissure line.[2] Direct comparison with CT, gross pathological and histological evaluations would help to determine which is the case. Some fissures were not visualised on all sequences and thin hypointense fissure lines were sometimes best appreciated on transverse slices. It is likely that some very thin fissure lines are not visible on low-field MRI due to inherent limitations of image resolution, in which case only the densification and bone oedema-like signal would be appreciated and result in a classification of 4a.[23] At the most severe end of the classifications, no cases were classified as 6 (complete fracture) likely because horses with complete fractures tend to be diagnosed with radiography and preferentially undergo CT for pre-operative planning.

There was no significant difference in the SGD MRI classifications, sub-classifications or extent of bone oedema-like signal between lame and non-lame limbs, and both groups included classifications of 4a, 4b and 5. The majority of horses with classification 4c and 5 were lame however one with a macrofissure was presented without lameness and in full competition training. Although the study did not directly take into account presence of pathology in other areas that may have contributed a greater extent to lameness, these findings reiterate the undependable nature of clinical lameness examinations for measuring the severity of SGD, as it is often intermittent.[3,6,12] Some horses were referred initially only for foot MRI due to a positive response to diagnostic analgesia of the foot. Consideration should always be given to performing a screening protocol for lesions in P1 if pathology explaining the lameness are not found in the foot in such cases.[5,6,28] Out of the 66 limbs that also had a foot MRI performed, seven had an SGD classification of 4c and 10 were classified as 5.

Dorsoproximal periosteal new bone formation on P1 is regarded as a prodromal sign of sagittal fissures but is inconsistently identified, reported to be less frequently visualised in radiographic examination than in CT, and has been infrequently reported in MRI of SGD.[1,2,5,6,11,12] In the present study, a confident identification of dorsal periosteal new bone was only made in limbs with relatively higher classifications of 4a, 4b and 5 (2.9%, 12% and 26.1% of limbs within those classifications, respectively). Periosteal new bone was rarely identified palmarly/plantarly, and only confidently identified in one limb with classification 5, in which the fissure extended to the plantar cortex. Due to blurred margins of cortical surfaces (due to volume averaging or motion), it is possible that these numbers are under- or overestimates of the true prevalence. Identification of periosteal new

bone on MRI needs to be further investigated to establish reliability, for example, via multimodality comparisons with CT and intra- and interobserver variability studies.

Periosteal oedema-like signal has not previously been described in equine MRI but is described in human tibial stress injuries where it is referred to as periosteal oedema.[17,18] Periosteal oedema-like signal in this study was identified as STIR FSE hyperintensity of the outer surface of the dorsoproximal and/or palmaro/plantaroproximal cortices. It was more difficult to assess periosteal oedema-like signal at the palmaro/plantaroproximal aspect of P1 due to the adjacent fetlock joint recess. Limbs with classification 5 proportionally had the highest prevalence of periosteal oedema-like signal both dorsally (confidently identified in 52.2%) and palmarly/plantarly (confidently identified in 4.3%).

While all limbs with confidently identified dorsal periosteal new bone also had confidently identified periosteal oedema-like signal, some horses without periosteal new bone formation had periosteal oedema-like signal. In some cases, this may indicate periosteal strain or inflammation which has not yet given rise to new bone formation. Although data on the following was not collected, it was frequently observed that there was a STIR FSE hyperintensity of the periosseous soft tissues at the dorsoproximal aspect of P1 in limbs with SGD. It is possible that this indicates increased vascularisation or oedema of the subcutaneous connective tissues. Further histological research is required to establish whether periosteal oedema-like signal as identified in this study represents periosteal or cortical oedema, another pathological process or whether it may be artefactual (volume averaging or motion).

Although dorsal periosteal new bone and oedema-like signal were identified more frequently in horses presenting with lameness than those without lameness, there was not a statistically significant difference ($p = 0.07$ and $p = 0.3$, respectively). Periostitis in tibial stress injuries in human patients is reported to be painful on palpation and contributes to problems with ambulation during exercise.[17] Similarly, palpation of the dorsoproximal aspect of P1 in horses with SG fissures is sometimes reported to illicit a pain response, however the contribution of periostitis in this region to lameness is not currently known.[4,12] Since the mammalian periosteum is more densely innervated with sensory and sympathetic fibres than bone marrow or cortex,[29] it is possible that certain phases of periosteal inflammation and remodelling could contribute to the varying severity of lameness in horses with SGD and this should be further investigated. Periosteal new bone and oedema-like signal were not included in the SGD classification system, however, if further research indicates that their presence or absence affects clinical outcomes then they may need to be integrated.

Increased size and/or number of vascular channels in the distal physeal region of the third metacarpus have been associated with subchondral bone injuries.[27] Increased vascular channels in the proximal aspect of P1 were most prevalent in SGD classification 5 and therefore are considered likely to develop secondary to inflammation and be associated with increased chronicity and severity of pathology.

Similar to previous reports, forelimbs were diagnosed more commonly than hindlimbs and in similar proportions regardless of whether they jumped or not.[2,3,5,6,8] In horses with bilateral forelimb SGD, 61% had different classifications in each limb. Most horses did not have more than one limb scanned but it is possible that there might be some level of SG changes bilaterally in a proportion of horses, though these may not necessarily be clinically important.[3,6]

It has been shown that complete fractures most often either extend into the proximal interphalangeal joint or to the lateral cortex of P1.[8,13] Similarly, in this sample microfissures and macrofissures most often coursed straight distally in a sagittal plane from the mid-sagittal region, with the second most common orientation being a lateral oblique one. Interestingly, although the majority of osseous densification and oedema-like signal was similarly centred sagittally, the second most common distribution was a centre toward medial. Recent investigation into strain parameters of the metacarpophalangeal joint indicate that the predominant biomechanical contributor to sagittal fracture of P1 are shear forces[15] and these medially and laterally directed changes possibly reflect the forces in effect which may vary dependent on individual anatomy and/or discipline.

Limitations of the study include those related to the nature of the referral caseload such as inconsistent amount of clinical information available for each horse and the absence of standardised diagnostic analgesia, and it therefore remains impossible to establish the origin of the lameness. Selection bias resulted in a study sample consisting predominantly of warmbloods used for showjumping and dressage as this reflects the large caseload of high-level sport horses at the diagnostic imaging centre at Equitom Equine Clinic. Inclusion was based on original MRI reports rather than a review of all images, which may contribute to selection bias and potentially under-representation of some classification types. Grading of images was challenging in some cases due to decreased image quality (e.g., movement artefact) or different arrays of acquired MRI sequences, however, this does reflect the normal clinical scenario of standing low-field MRI in the equine patient. The majority of image evaluations were performed by one blinded observer. To decrease the chance of erroneous evaluation, the grading data was cross-checked with the original report and a second blinded observer re-evaluated any discrepancies. Intra-observer and inter-observer variability should be tested to ensure repeatability and reproducibility in both the semi-quantitative grading scheme and classification systems.[16] Multiple differences were found between the original reports and blinded grading for the described level of severity of lesions (e.g., mild, moderate, severe). This is likely because the clinical history and clinical examination findings are normally taken into consideration while reporting on diagnostic images and that the markers of severity might be used differently in daily practice. A consistent and clinically relevant standardised grading scheme could limit such discrepancies.

To conclude, the proposed SGD MRI classification system is a useful means to describe severity of SGD. Future investigation should include prospective studies with multiple observers and populations of horses, and comparison with other imaging modalities. If the grades within the classification system correlate with clinical outcome, it

could be useful for longitudinal monitoring and assist in risk-assessment, formulating prognoses, creating rehabilitation programs and predicting the time to return to sports activity.

AUTHOR CONTRIBUTIONS

Josephine E. Faulkner: Conceptualization; data curation; formal analysis; investigation; methodology; project administration; resources; software; validation; visualization; writing – original draft; writing – review and editing. **Zoë Joostens:** Conceptualization; data curation; investigation; methodology; project administration; resources; software; supervision; validation; writing – review and editing. **Bart J. G. Broeckx:** Data curation; formal analysis; resources; software; supervision; validation; writing – review and editing. **Stijn Hauspie:** Data curation; investigation; resources; supervision; validation; writing – review and editing. **Tom Mariën:** Conceptualization; project administration; resources; software; supervision; validation; writing – review and editing. **Katrien Vanderperren:** Conceptualization; investigation; methodology; project administration; resources; supervision; validation; writing – review and editing.

FUNDING INFORMATION

No funding was received for this research.

CONFLICT OF INTEREST STATEMENT

No competing interests have been declared.

DATA INTEGRITY STATEMENT

Josephine E. Faulkner had full access to all the data in the study and takes responsibility for the integrity of the data and the accuracy of the data analysis.

ETHICAL ANIMAL RESEARCH

Research ethics committee oversight not required by this journal: retrospective study of clinical records.

INFORMED CONSENT

Explicit owner consent for animals' inclusion in the study was not stated.

PEER REVIEW

The peer review history for this article is available at https://www.webofscience.com/api/gateway/wos/peer-review/10.1111/evj.14088.

DATA AVAILABILITY STATEMENT

The data that support the findings of this study are available from the corresponding author upon reasonable request: Open sharing exemption granted by editor for this retrospective data analysis.

ORCID

Josephine E. Faulkner https://orcid.org/0000-0003-2597-4007
Zoë Joostens https://orcid.org/0000-0003-0116-4499

REFERENCES

1. Kuemmerle JM, Auer JA, Rademacher N, Lischer CJ, Bettschart-Wolfensberger R, Fürst AE. Short incomplete sagittal fractures of the proximal phalanx in ten horses not used for racing. Vet Surg. 2008;37(2):193–200. https://doi.org/10.1111/j.1532-950X.2007.00359.x
2. Brünisholz HP, Hagen R, Fürst AE, Kuemmerle JM. Radiographic and computed tomographic configuration of incomplete proximal fractures of the proximal phalanx in horses not used for racing. Vet Surg. 2015;44(7):809–15. https://doi.org/10.1111/vsu.12364
3. Gold SJ, Werpy NM, Gutierrez-Nibeyro SD. Injuries of the sagittal groove of the proximal phalanx in warmblood horses detected with low-field magnetic resonance imaging: 19 cases (2007–2016). Vet Radiol Ultrasound. 2017;58(3):344–53. https://doi.org/10.1111/vru.12488
4. Mizobe F, Nomura M, Ueno T, Yamada K. Bone marrow oedema-type signal in the proximal phalanx of thoroughbred racehorses. J Vet Med Sci. 2019;81(4):593–7. https://doi.org/10.1292/jvms.18-0530
5. Lipreri G, Bladon BM, Giorio ME, Singer ER. Conservative versus surgical treatment of 21 sports horses with osseous trauma in the proximal phalangeal sagittal groove diagnosed by low-field MRI. Vet Surg. 2018;47(7):908–15. https://doi.org/10.1111/vsu.12936
6. Dyson S, Nagy A, Murray R. Clinical and diagnostic imaging findings in horses with subchondral bone trauma of the sagittal groove of the proximal phalanx. Vet Radiol Ultrasound. 2011;52(6):596–604. https://doi.org/10.1111/j.1740-8261.2011.01852.x
7. Curtiss AL, Ortved KF, Dallap-Schaer B, Gouzeev S, Stefanovski D, Richardson DR, et al. Validation of standing cone beam computed tomography for diagnosing subchondral fetlock pathology in the Thoroughbred racehorse. Equine Vet J. 2021;53(3):510–23. https://doi.org/10.1111/evj.13414
8. Smith MRW, Wright IM. Radiographic configuration and healing of 121 fractures of the proximal phalanx in 120 Thoroughbred racehorses (2007-2011). Equine Vet J. 2014;46(1):81–7. https://doi.org/10.1111/evj.12094
9. Powell S. Low-field standing magnetic resonance imaging findings of the metacarpo/metatarsophalangeal joint of racing Thoroughbreds with lameness localised to the region: a retrospective study of 131 horses. Equine Vet J. 2012;44(2):169–77. https://doi.org/10.1111/j.2042-3306.2011.00389.x
10. Markel MD, Richardson DW. Noncomminuted fractures of the proximal phalanx in 69 horses. J Am Vet Med Assoc. 1985;186(6):573–9.
11. Smith MRW, Wright IM. Are there radiologically identifiable prodromal changes in Thoroughbred racehorses with parasagittal fractures of the proximal phalanx? Equine Vet J. 2014;46(1):88–91. https://doi.org/10.1111/evj.12093
12. Ramzan PHL, Powell SE. Clinical and imaging features of suspected prodromal fracture of the proximal phalanx in three Thoroughbred racehorses. Equine Vet J. 2010;42(2):164–9. https://doi.org/10.2746/042516409X478695
13. Holcombe S, Schneider R, Bramlage L, Gabel A, Bertone A, Beard W. Lag screw fixation of noncomminuted sagittal fractures of the proximal phalanx in racehorses: 59 cases (1973-1991). J Am Vet Med Assoc. 1995;206(8):1195–9.
14. Noble P, Singer ER, Jeffery NS. Does subchondral bone of the equine proximal phalanx adapt to race training? J Anat. 2016;229(1):104–13. https://doi.org/10.1111/joa.12478
15. Singer E, Garcia T, Stover S. How does bone strain vary between the third metacarpal and the proximal phalangeal bones of the equine distal limb? J Biomech. 2021;123:1–9. https://doi.org/10.1016/j.jbiomech.2021.110455
16. Olive J, D'anjou MA, Alexander K, Laverty S, Theoret C. Comparison of magnetic resonance imaging, computed tomography, and radiography for assessment of noncartilaginous changes in equine

metacarpophalangeal osteoarthritis. Vet Radiol Ultrasound. 2010; 51(3):267–79. https://doi.org/10.1111/j.1740-8261.2009.01653.x
17. Fredericson M, Bergman AG, Hoffman KL, Dillingham MS. Tibial stress reaction in runners correlation of clinical symptoms and scintigraphy with a new magnetic resonance imaging grading system. Am J Sports Med. 1995;23(4):472–81.
18. Kijowski R, Choi J, Shinki K, Del Rio AM, De Smet A. Validation of MRI classification system for tibial stress injuries. Am J Roentgenol. 2012;198(4):878–84. https://doi.org/10.2214/AJR.11.6826
19. Faulkner JE, Joostens Z, Broeckx BJG, Hauspie S, Mariën T, Vanderperren K. Follow-up magnetic resonance imaging of sagittal groove disease of the equine proximal phalanx using a classification system in 29 non-racing sports horses. Animals. 2023;14(1):34. https://doi.org/10.3390/ani14010034
20. Olive J, Serraud N, Vila T, Germain JP. Metacarpophalangeal joint injury patterns on magnetic resonance imaging: a comparison in racing Standardbreds and Thoroughbreds. Vet Radiol Ultrasound. 2017; 58(5):588–97. https://doi.org/10.1111/vru.12512
21. Smith MA, Dyson SJ, Murray RC. Reliability of high- and low-field magnetic resonance imaging systems for detection of cartilage and bone lesions in the equine cadaver fetlock. Equine Vet J. 2012;44(6): 684–91. https://doi.org/10.1111/j.2042-3306.2012.00561.x
22. Ross MW. Scintigraphic and clinical findings in the Standardbred metatarsophalangeal joint: 114 cases (1993-1995). Equine Vet J. 1998;30(2): 131–8. https://doi.org/10.1111/j.2042-3306.1998.tb04472.x
23. Lin ST, Foote AK, Bolas NM, Peter VG, Pokora R, Patrick H, et al. Three-dimensional imaging and histopathological features of third metacarpal/tarsal parasagittal groove and proximal phalanx sagittal groove fissures in thoroughbred horses. Animals. 2023;13:2912. https://doi.org/10.3390/ani13182912
24. De Guio C, Ségard-Weisse E, Thomas-Cancian A, Schramme M. Bone marrow lesions of the distal condyles of the third metacarpal bone are common and not always related to lameness in sports and pleasure horses. Vet Radiol Ultrasound. 2019;60(2):167–75. https://doi.org/10.1111/vru.12700
25. Smith MA, Dyson SJ. Normal MRI anatomy: The fetlock region. In: Murray R, editor. Equine MRI. Chichester, UK: John Wiley & Sons Ltd; 2010. p. 173–89. https://doi.org/10.1002/9781118786574.ch6
26. Murray R, Werpy N. Principles of MRI in horses: Image interpretation and artefacts. In: Murray R, editor. Equine MRI. Chichester, UK: John Wiley & Sons Ltd; 2010. p. 101–45. https://doi.org/10.1002/9781118786574.ch4
27. Powell S. Pathology: The fetlock region. In: Murray RC, editor. Equine MRI. Chichester, UK: John Wiley & Sons Ltd; 2010. p. 315–59. https://doi.org/10.1002/9781118786574.ch13
28. Nagy A, Malton R. Diffusion of radiodense contrast medium after perineural injection of the palmar digital nerves. Equine Vet Educ. 2015;27(12):648–54. https://doi.org/10.1111/eve.12369
29. Steverink JG, Oostinga D, van Tol FR, van Rijen MHP, Mackaaij C, Verlinde-Schellekens SAMW, et al. Sensory innervation of human bone: an immunohistochemical study to further understand bone pain. J Pain. 2021;22(11):1385–95. https://doi.org/10.1016/j.jpain.2021.04.006

SUPPORTING INFORMATION

Additional supporting information can be found online in the Supporting Information section at the end of this article.

How to cite this article: Faulkner JE, Joostens Z, Broeckx BJG, Hauspie S, Mariën T, Vanderperren K. Low-field magnetic resonance imaging of sagittal groove disease of the proximal phalanx in non-racing sport horses. Equine Vet J. 2024. https://doi.org/10.1111/evj.14088